



## OPEN Efficacy of silver-doped Carbon dots in Chemical Castration: a rat model study

Ali Soleimanzadeh<sup>1</sup>✉, Niki Karvani<sup>1</sup>, Farshid Davoodi<sup>2</sup>✉, Rahim Molaie<sup>3</sup> & Abbas Raisi<sup>4</sup>

This study evaluates silver-doped carbon dots (AgCDs) as a novel agent for chemical castration using a rat model. Six groups of rats (five males and ten females each, except for the surgical group which had only males) were utilized to compare the effects of different concentrations of AgCDs. The groups included control, sham, and three experimental groups injected with 1.25, 50, and 200 µg/mL AgCDs, respectively, along with a surgical castration group. Testosterone levels, sperm parameters, fertility index, oxidative damage, histopathological parameters, and gene expression of *P53*, *Bax*, *Bcl-2*, *caspase-3*, *AKT*, and *PI3K* were analyzed. Results demonstrated that the high-dose AgCDs group significantly reduced testosterone levels, sperm concentration, and motility, resulting in a decreased fertility index. MDA and NO significantly increased, while CAT, SOD, GPx, and TAC significantly reduced in the chemically castrated groups. Histological and genes expression analysis also revealed apoptosis and testicular damage in the AgCDs groups, indicated by significant increases in *P53*, *Bax*, and *Caspase-3* levels, and significant reductions in *AKT*, *PI3K*, and *Bcl-2*. Based on these findings, AgCDs could be considered a potent and efficient agent for chemical castration, offering a less invasive, cost-effective solution with potential applications for population control.

**Keywords** Chemical castration, Carbon dots, Silver, Sperm parameters, Oxidative stress, Rat

### Abbreviations

TM	Total motility
PM	Progressive motility
VCL	Curvilinear velocity
VSL	Straight-line velocity
VAP	Average path velocity
STR	Straightness
LIN	Linearity
ALH	Amplitude of lateral head displacement
BCF	Beat-cross frequency
PMF	Plasma membrane functionality
qRT-PCT	Quantitative reverse transcription polymerase chain reaction
TAC	Total antioxidant capacity
MDA	Malondialdehyde
CAT	Catalase
GPx	Glutathione peroxidase
SOD	Superoxide dismutase
NO	Nitric oxide
ROS	Reactive oxygen species

The sterilization of animals was preceded in 7000 BC. Castration is required to manage the overgrowth of canine populations, which leads to environmental health problems and zoonosis disease<sup>1</sup>. Additionally, it aids in curbing overpopulation by eliminating sexual and masculine behaviors<sup>2,3</sup>. Castration methods include chemical, hormonal, and surgical approaches<sup>4</sup>.

<sup>1</sup>Department of Theriogenology, Faculty of Veterinary Medicine, Urmia University, Urmia, Iran. <sup>2</sup>Department of Clinical Sciences, Faculty of Veterinary Medicine, Razi University, Kermanshah, Iran. <sup>3</sup>Fanavaran NanoZist Plast Co, Urmia, Iran. <sup>4</sup>Department of Clinical Sciences, Faculty of Veterinary Medicine, Lorestan University, Khorramabad, Iran. ✉email: a.soleimanzadeh@urmia.ac.ir; farshiddavoodi620@yahoo.com

While the surgical method has been employed for many years, it is expensive, risky, and time-consuming. Furthermore, the need for equipment, skilled veterinarians, and postoperative care puts it at a disadvantage<sup>1–3</sup>. On the other hand, hormonal castration can affect the target organ and harm non-targeted organs. Nowadays, chemical castration is preferred over surgical methods due to its low cost and easiness. Moreover, chemical sterilization reduces stress and the probability of bleeding, infection, hernia, and the number of staff during the castration process. Hence, it can be done in large populations quickly<sup>2,5</sup>. Furthermore, behavioral problems arising from androgens, which cannot be addressed through surgical methods, are alleviated through chemical sterilization<sup>6</sup>.

Different animal models have been studied, including stallions, donkeys, bucks, buffalo, cattle, goats, Mongolian gerbils, ferrets, frogs, cats, dogs and rodents like rats, and mice. Multiple agents like calcium chloride, clove oil, mannitol, glycerin, atrazine, sodium chloride, deslorelin, ethanol, iron (III) chloride hexahydrate, chlorhexidine gluconate, and cetrime, and formalin were employed in these studies<sup>2,6–12</sup>.

Carbon dots (CD), the latest addition to carbon nanomaterials, fall into the category of zero-dimensional carbon with a size smaller than 10 nm<sup>13</sup>. CDs possess a core that consists of sp<sup>2</sup> or sp<sup>3</sup> hybridized conjugated carbon. Furthermore, they have a shell that can include COOH, NH, OH, SH, C=O, C–O–C, C–N, and polymer aggregates<sup>13,14</sup>. Due to their unique features, including excellent solubility, favorable optical and physical properties, and excitation-dependent photoluminescence, CDs have recently become a focal point of significant interest. They can be utilized in different areas such as bioimaging, drug and gene delivery, sensing, catalysis, optoelectronics, and photo-dermal therapies<sup>13–15</sup>. Due to their small size, they can act alone or be combined with other nanotherapeutics for more functional capacities<sup>16</sup>. Many heteroatoms like sulfur, nitrogen, phosphorus, boron, and metals like Cu, Zn, Mg, Au, have been used as doping agents. It has been demonstrated that metal-doped CDs are superior electron donors and have more empty orbitals. Furthermore, they can enhance the quantum yield. Compared to immaculate CDs, metal-doped ones have higher optical absorbance and improved catalytic performance<sup>13</sup>. The toxicity of carbon dots was reported to be low<sup>15,17</sup>. However, we should consider the toxicity of any nanoparticle agent functionalized with toxic chemicals. It has been demonstrated that Ag2S QDs capped with DMSA had low toxicity in high doses, which caused apoptosis<sup>13,16</sup>. Moreover, nanocarbon dots have been used in various environmental demands, from water to air pollution, because of their high surface area, solubility, and large pore size<sup>18</sup>. In a study, CDs functionalized with nitrogen acted as antimicrobial and antibacterial in packaging effectively<sup>19</sup>. Moreover, selenium-doped carbon dots were employed for acute kidney injury in animal models, leading to increased cell viability due to decreased damage from oxidative stress<sup>20</sup>. Even though nanocarbon dots have proven helpful in various applications, their efficacy in castration has not been studied so far. Our study aims to evaluate the histology, oxidative stress, and different sperm parameters after administering silver-doped carbon dots in rats' chemical castration.

## Results

### Testosterone levels

The control and sham groups exhibited the highest levels of testosterone, with more than 1.70 ng/mL on day 60. The surgically castrated group showed the lowest level of testosterone, at  $0.31 \pm 0.02$  ng/mL. Administration of AgCDs significantly reduced testosterone levels compared to the control and sham groups ( $p \leq 0.05$ ). Among the chemically castrated groups, the 200 AgCDs group had the lowest testosterone levels, comparable to those of the surgically castrated group (Fig. 1).

### Sperm parameters

According to Table 1, no significant differences were observed for all evaluated parameters between the control and sham groups injected with normal saline ( $p > 0.05$ ). Significant differences were found in parameters including epididymal sperm concentration, total motility, VSL, and BCF in all AgCDs-injected groups compared to the control and sham groups ( $p < 0.05$ ). Additionally, significant differences were observed among all AgCDs-injected groups for these parameters ( $p < 0.05$ ). For parameters such as VAP, VCL, VSL, and ALH, no significant differences were observed between the sham group and the 1.25 AgCDs group. However, AgCDs injections at dosages of 50 and 200 µg/kg significantly reduced VAP, VCL, VSL, and ALH compared to the control and sham groups ( $p < 0.05$ ). No significant differences were observed among the various groups for LIN and STR ( $p > 0.05$ ) (Table 1).

Based on Table 2, AgCDs injections significantly reduced plasma membrane functionality, viability, DNA damage, and morphology compared to the control and sham groups ( $p < 0.05$ ) (Table 2).

### Fertility indexes

According to Table 3, there were ten females in each group. Although all ten females in each group mated, the number of males who mated was half in all groups. While five males impregnated all female rats in the control and sham groups, one female in the 1.25 AgCDs group did not become pregnant. The fertility index in the 50 AgCDs group decreased to 40%, with only 2 out of 5 males successfully impregnating females. Additionally, none of the males in the 200 AgCDs group could impregnate females. A significant difference in the pregnancy index was observed between the 50 and 200 AgCDs groups and the control and sham groups ( $p < 0.05$ ) (Table 3).

### Oxidative stress

Figure 2 represents the results for oxidative stress biomarkers. Based on the graph, no significant differences were observed between the sham and control groups for all evaluated biomarkers ( $p > 0.05$ ). In the chemically castrated groups, administration of AgCDs at various doses significantly increased the levels of MDA compared to the sham and control groups ( $p < 0.05$ ). Levels of NO significantly increased in the 50 and 200 AgCDs groups compared to the sham and control groups ( $p < 0.05$ ). AgCDs injections at different doses significantly reduced

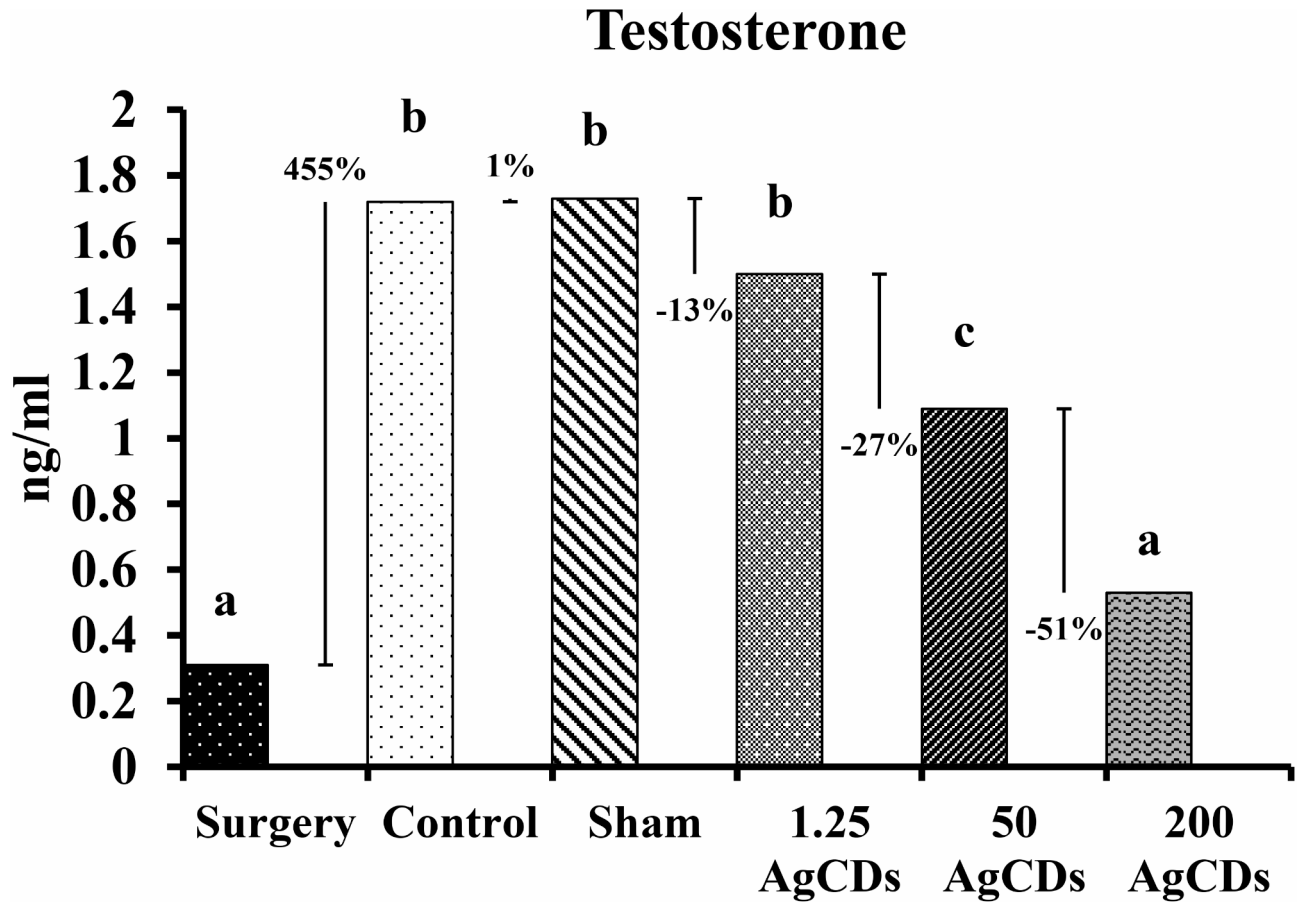


**Fig. 1.** Effect of intratesticular injection of AgCDs on serum testosterone concentration in experimental groups at day 60. (a–d) Various letters indicate significant differences between groups ( $p \leq 0.05$ ; mean  $\pm$  SEM).

Analysis	C	Sham	1.25 AgCDs	50 AgCDs	200 AgCDs
Epididymal sperm concentration ( $10^6$ /mL)	$37.2 \pm 34.38^a$	$37.1 \pm 29.91^a$	$33.25 \pm 24.96^b$	$25.31 \pm 28.24^c$	$7.14 \pm 31.09^d$
Total motility (%)	$82.64 \pm 3.32^a$	$80.51 \pm 2.64^a$	$72.50 \pm 2.11^b$	$58.36 \pm 2.35^c$	$20.88 \pm 1.47^d$
Progressive motility (%)	$47.20 \pm 1.48^a$	$45.05 \pm 1.62^{a,b}$	$39.31 \pm 1.50^b$	$27.48 \pm 1.34^c$	$1.68 \pm 0.09^d$
VAP ( $\mu$ m/s)	$31.09 \pm 1.86^a$	$29.84 \pm 1.82^{a,b}$	$27.47 \pm 1.33^b$	$22.25 \pm 1.95^c$	$10.60 \pm 1.01^d$
VCL ( $\mu$ m/s)	$86.88 \pm 3.91^a$	$85.58 \pm 3.65^{a,b}$	$82.88 \pm 2.88^b$	$73.47 \pm 2.13^c$	$40.85 \pm 1.51^d$
VSL ( $\mu$ m/s)	$23.54 \pm 1.44^a$	$23.17 \pm 1.75^a$	$21.19 \pm 1.83^b$	$15.73 \pm 1.89^c$	$9.60 \pm 1.45^d$
LIN (%)	$0.21 \pm 0.01^a$	$0.21 \pm 0.03^a$	$0.20 \pm 0.02^a$	$0.20 \pm 0.02^a$	$0.20 \pm 0.01^a$
ALH ( $\mu$ m/s)	$2.57 \pm 0.02^a$	$2.23 \pm 0.03^{a,b}$	$2.11 \pm 0.02^b$	$1.67 \pm 0.03^c$	$0.84 \pm 0.03^d$
STR (%)	$0.81 \pm 0.01^a$	$0.81 \pm 0.02^a$	$0.81 \pm 0.02^a$	$0.80 \pm 0.01^a$	$0.80 \pm 0.03^a$
BCF (Hz)	$13.40 \pm 1.85^a$	$13.15 \pm 1.07^a$	$12.83 \pm 1.91^b$	$10.38 \pm 1.36^c$	$5.89 \pm 0.78^d$

**Table 1.** Epididymal sperm concentration, total and progressive motilities and motility characteristics in different experimental groups. C control, AgCDs Silver Carbon nanodots, VAP Average path velocity, VCL Curvilinear velocity, VSL Straight line velocity, LIN Linearity, ALH Amplitude of lateral head displacement, STR Straightness, BCF Beat-cross frequency. <sup>a–d</sup>Different superscripts within the same row demonstrate significant differences ( $p \leq 0.05$ ; mean  $\pm$  SEM).

levels of CAT, SOD, GPx, and TAC compared to the sham and control groups ( $p < 0.05$ ). Furthermore, significant differences were observed among all AgCDs-injected groups, with the highest testicular damage in the 200 AgCDs group ( $p < 0.05$ ) (Fig. 2).

#### Macroscopic and histopathological assessment

Table 4 presents the results of macroscopic evaluations. Testis weight, starting at  $0.49 \pm 0.05$  g in the control group, showed a slight decrease in the sham group. When the testis was exposed to silver carbon dots, a weight

Analysis	C	Sham	1.25 AgCDs	50 AgCDs	200 AgCDs
Sperm plasma membrane functionality (%)	85.84 ± 2.92 <sup>a</sup>	83.53 ± 3.84 <sup>a,b</sup>	80.85 ± 2.81 <sup>b</sup>	61.80 ± 2.50 <sup>c</sup>	22.64 ± 1.10 <sup>d</sup>
Sperm viability (%)	92.69 ± 2.89 <sup>a</sup>	91.26 ± 3.51 <sup>a,b</sup>	88.47 ± 2.48 <sup>b</sup>	65.64 ± 3.42 <sup>c</sup>	26.09 ± 1.87 <sup>d</sup>
Sperm DNA damage (%)	2.43 ± 0.22 <sup>a</sup>	3.17 ± 0.29 <sup>a</sup>	5.82 ± 0.62 <sup>b</sup>	35.39 ± 0.81 <sup>c</sup>	61.88 ± 1.91 <sup>d</sup>
Sperm abnormal morphology (%)	5.90 ± 0.39 <sup>a</sup>	6.79 ± 0.38 <sup>a</sup>	8.10 ± 0.46 <sup>b</sup>	21.62 ± 0.62 <sup>c</sup>	52.69 ± 1.10 <sup>d</sup>

**Table 2.** Epididymal sperm plasma membrane functionality, DNA damage, viability and abnormal morphology in different experimental groups. C control, AgCDs Silver carbon nanodots. <sup>a–d</sup>Different superscripts within the same row demonstrate significant differences ( $p \leq 0.05$ ; mean  $\pm$  SEM).

Analysis	C	Sham	1.25 AgCDs	50 AgCDs	200 AgCDs
Number of females	10	10	10	10	10
Number of females mated	10	10	10	10	10
Number of males mated	5	5	5	5	5
Number of males impregnating females	5	5	5	2	0
Number of females pregnant	10	10	9	3	0
Female mating index (%)	100 <sup>a</sup>	100 <sup>a</sup>	100 <sup>a</sup>	100 <sup>a</sup>	100 <sup>a</sup>
Male mating index (%)	100 <sup>a</sup>	100 <sup>a</sup>	100 <sup>a</sup>	100 <sup>a</sup>	100 <sup>a</sup>
Pregnancy index (%)	100 <sup>a</sup>	100 <sup>a</sup>	90.00 <sup>b</sup>	30.00 <sup>c</sup>	0.00 <sup>d</sup>
Male fertility index (%)	100 <sup>a</sup>	100 <sup>a</sup>	100 <sup>a</sup>	40.00 <sup>b</sup>	0.00 <sup>c</sup>

**Table 3.** Fertility indexes of adult male rats after natural mating with non-exposed females. C control, AgCDs Silver carbon nanodots. Female mating index = number of females mated/number of females  $\times$  100; Male mating index = number of males mated/number of males  $\times$  100; Pregnancy index = number of females pregnant/number of females mated  $\times$  100; Male fertility index = number of males impregnating females/number of males mated  $\times$  100. <sup>a–d</sup>Different superscripts within the same row demonstrate significant differences ( $p \leq 0.05$ ; mean  $\pm$  SEM).

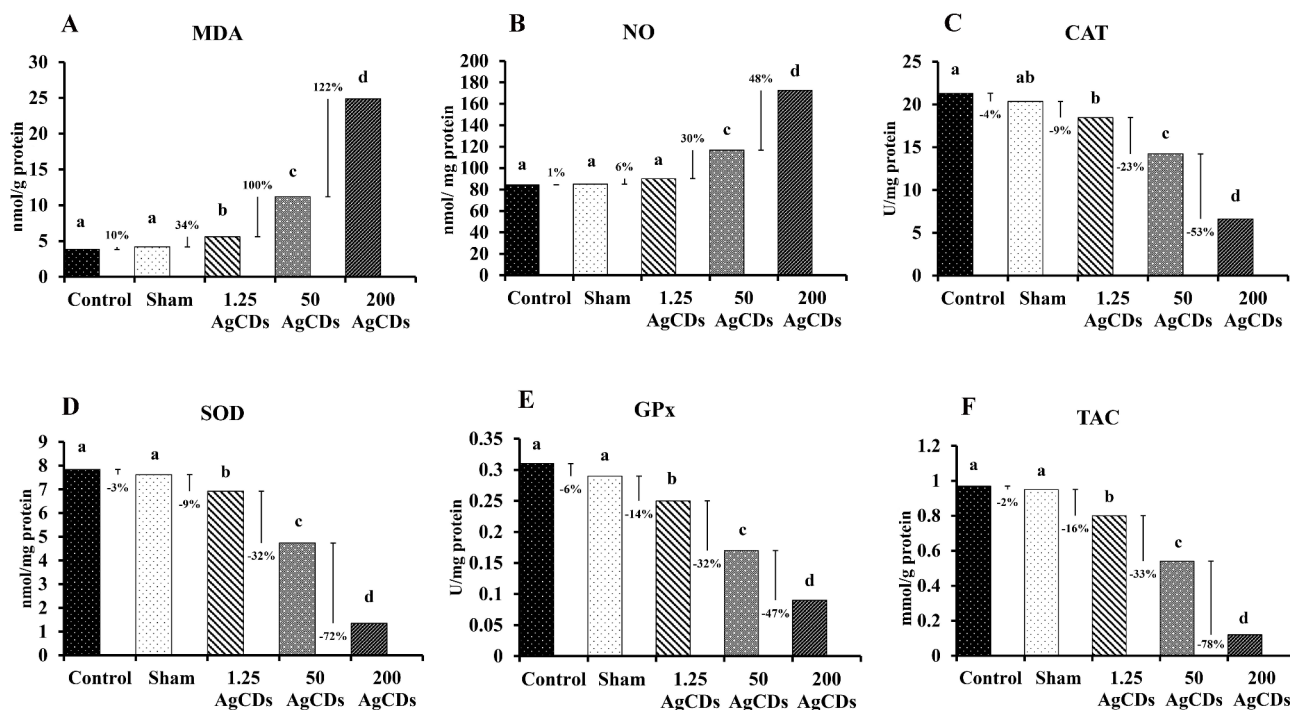


**Fig. 2.** Evaluation of oxidative stress biomarkers in different experimental groups of the study. (A) Malondialdehyde (MDA), (B) nitric oxide (NO), (C) catalase, (D) superoxide dismutase, (E) glutathione peroxidase, (F) total antioxidant capacity. a–d: Various letters indicate significant differences between groups ( $p \leq 0.05$ ; mean  $\pm$  SEM).

Analysis	C	Sham	1.25 AgCDs	50 AgCDs	200 AgCDs
Testis weight (g)	0.49 ± 0.05 <sup>a</sup>	0.46 ± 0.03 <sup>a</sup>	0.38 ± 0.03 <sup>b</sup>	0.25 ± 0.04 <sup>c</sup>	0.09 ± 0.01 <sup>d</sup>
Epididymis weight (g)	0.215 ± 0.01 <sup>a</sup>	0.208 ± 0.01 <sup>a</sup>	0.184 ± 0.01 <sup>b</sup>	0.110 ± 0.01 <sup>c</sup>	0.051 ± 0.01 <sup>d</sup>
Testis/body weight (%)	1.962 ± 0.03 <sup>a</sup>	1.961 ± 0.05 <sup>a</sup>	1.527 ± 0.12 <sup>b</sup>	1.086 ± 0.10 <sup>c</sup>	0.375 ± 0.04 <sup>d</sup>
Johnsen score	9.26 ± 0.57 <sup>a</sup>	9.10 ± 0.83 <sup>a</sup>	8.71 ± 0.58 <sup>b</sup>	5.25 ± 0.51 <sup>c</sup>	1.07 ± 0.06 <sup>d</sup>
Cosentino score	1.02 ± 0.13 <sup>a</sup>	1.07 ± 0.15 <sup>a</sup>	1.29 ± 0.11 <sup>b</sup>	2.31 ± 0.16 <sup>c</sup>	3.45 ± 0.11 <sup>d</sup>
Seminiferous tubule diameter (STsD) (µm)	311.23 ± 2.71 <sup>a</sup>	306.41 ± 3.54 <sup>a</sup>	287.62 ± 2.91 <sup>b</sup>	253.93 ± 1.72 <sup>c</sup>	198.47 ± 1.46 <sup>d</sup>
Sertoli cell index (SCI)	13.22 ± 1.08 <sup>a</sup>	13.43 ± 1.32 <sup>a</sup>	10.83 ± 0.36 <sup>b</sup>	8.97 ± 0.88 <sup>c</sup>	7.27 ± 0.67 <sup>d</sup>
Repopulation index (RI)	80.17 ± 2.31 <sup>a</sup>	78.09 ± 2.31 <sup>a,b</sup>	75.27 ± 2.45 <sup>b</sup>	57.44 ± 1.53 <sup>c</sup>	30.89 ± 1.16 <sup>d</sup>
Miotic index (MI)	2.96 ± 0.15 <sup>a</sup>	2.84 ± 0.09 <sup>a</sup>	2.55 ± 0.14 <sup>b</sup>	1.98 ± 0.20 <sup>c</sup>	1.01 ± 0.04 <sup>d</sup>
Leydig cell nuclear diameter (LCND)(µm)	7.12 ± 0.85 <sup>a</sup>	7.30 ± 0.38 <sup>a</sup>	7.96 ± 0.45 <sup>b</sup>	9.81 ± 0.56 <sup>c</sup>	11.24 ± 0.80 <sup>d</sup>
Tubular differentiation index (TDI)(%)	82.29 ± 3.17 <sup>a</sup>	79.68 ± 2.56 <sup>a,b</sup>	75.45 ± 2.79 <sup>b</sup>	67.95 ± 2.09 <sup>c</sup>	57.92 ± 1.13 <sup>d</sup>
Spermiogenesis index (SPI)(%)	80.23 ± 2.65 <sup>a</sup>	77.66 ± 3.37 <sup>a</sup>	73.71 ± 2.67 <sup>b</sup>	61.46 ± 1.36 <sup>c</sup>	45.20 ± 1.79 <sup>d</sup>

**Table 4.** Histological parameters and reproductive organ weights in different experimental groups. C control, AgCDs Silver carbon nanodots. <sup>a-f</sup>Different superscripts within the same row demonstrate significant differences ( $p \leq 0.05$ ; mean  $\pm$  SEM).

loss was observed in the 1.25 AgCDs, 50 AgCDs, and 200 AgCDs groups. Similarly, epididymis weight followed the same trend, showing a significant loss, falling below 0.1 g in the 200 AgCDs group compared to the control group ( $p < 0.05$ ). The testis weight to body weight ratio was almost the same in the control and sham groups; however, the percentage was significantly reduced in the carbon dots-injected groups ( $p < 0.05$ ). H&E slides for testicular tissue in all experimental groups are presented at Fig. 3. Based on Fig. 3, the highest tissue destruction and emptying of testicular tubules were observed in the group with high dose of AgCDs.

The results of all histological parameters are presented in Table 4. According to Johnsen's score, the control group had the highest level of spermatogenesis. In contrast, there was a significant drop in the carbon dots-treated groups, reaching almost a score of 1 (very low to zero germ cells) in the 200 AgCDs group. On the other hand, the Cosentino score indicated a gradual increase with higher doses of carbon dots, with the 200 AgCDs group exhibiting the most testicular damage and receiving a grade of more than 3. There was a significant decline in the levels of all histological parameters from the control group to the high-dose carbon dot group, except for LCND ( $p < 0.05$ ). The analysis of LCND (µm) showed a significant increase in diameter due to the damage caused by carbon dots to the testes ( $p < 0.05$ ) (Table 4).

#### qRT-PCR

The mRNA expression of *P53*, *Bax*, and *caspase-3* increased significantly and dose-dependently with silver carbon dots, while the expression of *AKT*, *PI3K*, and *Bcl-2* significantly decreased in the AgCDs-administered groups compared to the sham and control groups ( $p < 0.05$ ) (Table 5).

#### Discussion

In this research, we studied the utilization of carbon dots in the chemical castration of male rats (Fig. 4). Chemical castration has been used in various studies, and different parameters of the sperm have been investigated. Motility is one of the essential characteristics of a normal spermatozoa<sup>21</sup>. Jung and Yoon (2017) researched injecting 70% glycerin into the testicles of a stallion and found that it can reduce the total motile sperm<sup>22</sup>. Another study demonstrated that there are two pathways controlling the motility of spermatozoa, which are the calcium ( $Ca^{2+}$ ) pathway and the cyclic adenosine monophosphate (cAMP)-dependent protein kinase or protein kinase A (PKA) pathway<sup>23</sup>. In a study, the administration of sodium chloride solution into the testes of male cats led to inconvenience in those two pathways, and as a result, it lowered sperm motility<sup>10</sup>. Another research performed by Mohammad and James indicated that the motility of sperm cells was 60 to 80% before intratesticular injection of chlorhexidine gluconate and cetrime in bucks; however, it lowered to zero, and poor motility was detected three days following injection<sup>24</sup>. Oliveira et al.<sup>25</sup> investigated the effects of intratesticular injection of zinc gluconate-based solution in dogs, and their results revealed a significant decrease in sperm motility<sup>25</sup>. The present study's findings are consistent with those of previous studies, which show that intratesticular injection of silver-doped carbon dots significantly reduced the motility of spermatozoa in rats. DNA fragmentation was also evaluated in earlier studies as an essential parameter. In an investigation on chemical castration in a rat model using an intratesticular injection of mannitol, Carnoy's fixative was employed for the fixation of sperm cells, followed by acridine-orange staining. The findings of the mentioned study revealed that the percentage of sperms with fragmented DNA significantly increased<sup>2</sup>. Not only was the DNA of sperm studied in chemical castration but the effect of heavy quantum dots was also studied. Previous studies demonstrated that nanomaterials induce oxidative stress and elevate reactive oxygen species (ROS). ROS leads to DNA damage and destruction of the cell membrane in spermatozoa, which can lead to infertility in male<sup>26</sup>.

The cytotoxicity of carbon dots is affected by different parameters such as particle size, stability, surface coating and functionalization, and aggregation<sup>27</sup>. The findings of the study conducted by Habiba et al.<sup>28</sup> indicated that the cell viability of normal mammalian cells treated with bare Ag-NPs was significantly reduced<sup>28</sup>. The toxicity of silver carbon dots on aquatic species such as zebrafish indicated that their toxicity depends on



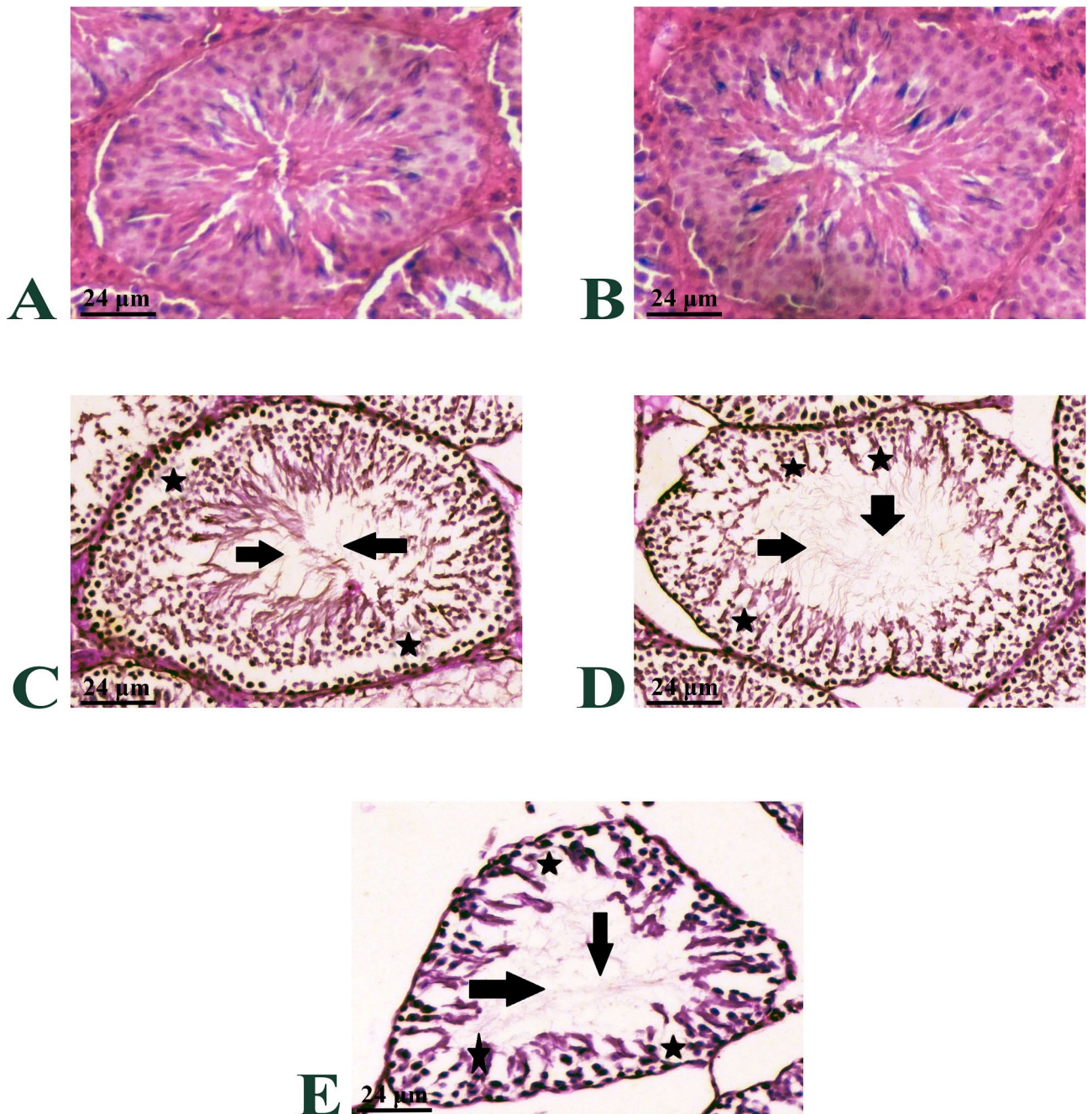


**Fig. 3.** Testicular histo-architecture was compared across different experimental groups: (A) control; (B) Sham; (C) 1.25 µg/kg AgCDs; (D) 50 µg/kg AgCDs; (E) 200 µg/kg AgCDs. Hematoxylin and eosin (H&E) staining at 400× magnification was used. The black arrows indicate sperm density in seminiferous tubules lumen, being reduced particularly in group E, also observed in groups C and D. Groups C, D, and E showed toxic effects of the substance used. The asterisks indicate germinal epithelium disorganization and disruption among different groups, being particularly severe in group E, but also observed in groups C and D.

their concentration<sup>29</sup>. The signs of toxicity in zebrafish were bradycardia, high mortality rate, and hatching time delays in embryos. Carbon dots in concentrations lower than 200 µg mL<sup>-1</sup> trigger mortality of 80% of living cells over 24 h. Regardless of whether binding toxic ligands to carbon dots have reduced toxicity, certain factors may trigger undesired reactions in the body. These include administering multiple doses, concentrating charge densities in specific areas, having a hydrodynamic diameter above 6 nanometers, maintaining a higher positive charge, and getting activated by extended light irradiation<sup>16</sup>. In a study, DMSA-capped Ag2S quantum dots were not cytotoxic or genotoxic unless in high doses, which caused apoptosis in cells<sup>30</sup>.

A study conducted by Maadi et al. (2023) examined testosterone concentration in chemically castrated rats using hypertonic saline, revealing a significant reduction compared to baseline values<sup>2</sup>. Another study using

Analysis	C	Sham	1.25 AgCDs	50 AgCDs	200 AgCDs
<i>P53</i> (Fold change)	1.03 ± 0.05 <sup>a</sup>	1.05 ± 0.04 <sup>a</sup>	1.12 ± 0.07 <sup>b</sup>	1.27 ± 0.12 <sup>c</sup>	1.65 ± 0.10 <sup>d</sup>
<i>Bax</i> (Fold change)	0.70 ± 0.03 <sup>a</sup>	0.75 ± 0.03 <sup>a</sup>	0.83 ± 0.05 <sup>b</sup>	1.02 ± 0.09 <sup>c</sup>	1.37 ± 0.14 <sup>d</sup>
<i>Caspase-3</i> (Fold change)	0.84 ± 0.04 <sup>a</sup>	0.88 ± 0.03 <sup>a</sup>	0.97 ± 0.04 <sup>b</sup>	1.15 ± 0.11 <sup>c</sup>	1.34 ± 0.07 <sup>d</sup>
<i>AKT</i> (Fold change)	0.93 ± 0.05 <sup>a</sup>	0.91 ± 0.02 <sup>a</sup>	0.85 ± 0.07 <sup>b</sup>	0.63 ± 0.05 <sup>c</sup>	0.34 ± 0.03 <sup>d</sup>
<i>PI3K</i> (Fold change)	1.07 ± 0.07 <sup>a</sup>	1.06 ± 0.06 <sup>a</sup>	0.82 ± 0.05 <sup>b</sup>	0.54 ± 0.06 <sup>c</sup>	0.29 ± 0.02 <sup>d</sup>
<i>Bcl-2</i> (Fold change)	0.97 ± 0.05 <sup>a</sup>	0.93 ± 0.04 <sup>a</sup>	0.87 ± 0.06 <sup>b</sup>	0.73 ± 0.04 <sup>c</sup>	0.45 ± 0.05 <sup>d</sup>

**Table 5.** The mRNA expression levels using semiquantitative reverse transcription-polymerase chain reaction (RT-PCR). C control, AgCDs Silver carbon nanodots. The density of *P53*, *Bax*, *Caspase-3*, *PI3K*, and *Bcl-2* mRNA levels in testicular tissue was measured by densitometry and normalized to the *18SrRNA* mRNA expression level. <sup>a-d</sup>Different superscripts within the same row demonstrate significant differences ( $p \leq 0.05$ ; mean ± SEM).

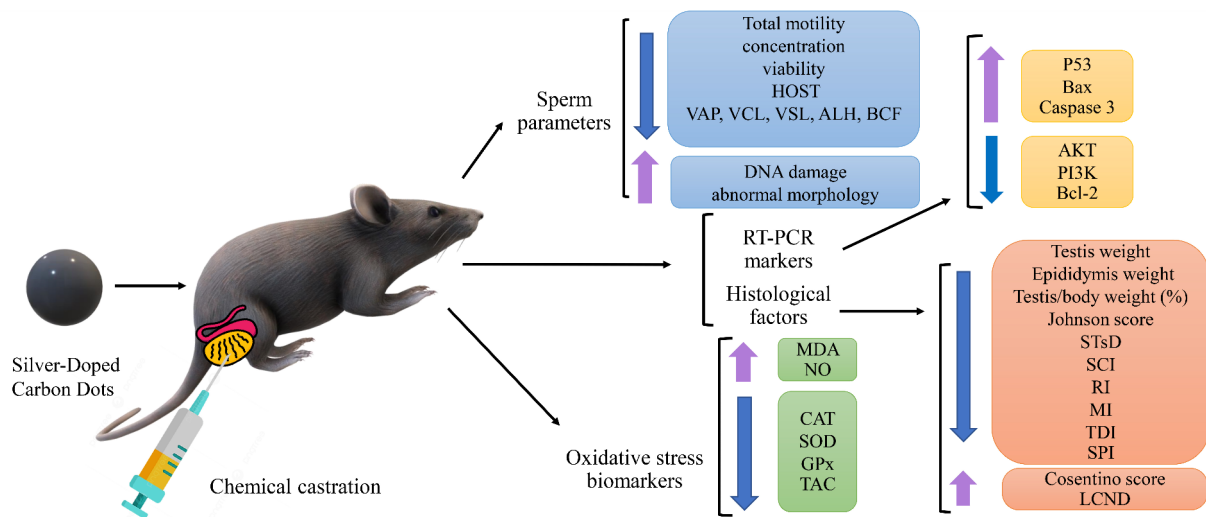


**Fig. 4.** Using silver-doped carbon dots as an agent for chemical castration. Silver-doped carbon dots reduced sperm parameters such as total motility, concentration, viability, HOST, VAP, VCL, VSL, ALH, and BCF. Furthermore, DNA damage and abnormal morphology of spermatozoa increased. Levels of *P53*, *Bax*, and *Caspase-3* increased and levels of *AKT*, *PI3K*, and *Bcl-2* reduced in the qRT-PCR analysis. All the measured histopathological parameters decreased except the Cosentino's score and LCND which increased. MDA and NO significantly increased in the rats that received AgCDs and parameters such as CAT, SOD, GPx, and TAC decreased.

an intratesticular injection of 20% hypertonic saline also indicated a significant reduction in testosterone levels compared to baseline values<sup>31</sup>. Calcium chloride, another agent used for chemical castration, decreased testosterone levels compared to the control group<sup>8</sup>. Consistent with the findings of previous studies, the present study showed a significant reduction in testosterone levels in the chemically castrated groups.

In the present study, injection of AgCDs significantly increased levels of MDA and NO and reduced levels of CAT, SOD, GPx, and TAC compared to the sham and control groups ( $p < 0.05$ ). These findings align with those of Moustafa et al. (2023), who demonstrated that chemical castration using formalin in dogs led to a significant increase in MDA and NO levels and a reduction in GSH levels<sup>12</sup>. Similarly, Karami et al. (2023) assessed the effects of calcium chloride in chemical castration and reported significant reductions in SOD and GPx levels compared to the sham group<sup>32</sup>.

In a study on the effects of intratesticular injection of mannitol for chemical castration, results indicated that Johnson's score and SPI significantly decreased compared to the intact group ( $p < 0.05$ ). Additionally, depletion of seminiferous tubules, vacuolization, atrophy, multinucleated giant cell formation, and testicular congestion were observed in the mannitol-injected group<sup>2</sup>. Another study examined the effects of intratesticular injection of hypertonic saline for chemical castration in rats, showing that it was associated with tubular degeneration and immune cell infiltration<sup>33</sup>. A zinc-based solution combined with anti-inflammatory and analgesic drugs was used for chemical sterilization in rats, resulting in a significant reduction in testicular and epididymal weight<sup>34</sup>. Consistent with these previous studies, the present study found that intratesticular injection of AgCDs significantly reduced testicular and epididymis weight, as well as other histopathological parameters including STsD, SCI, RI, MI, TDI, and SPI.

While Silver-Doped Carbon Dots (Ag-CDs) have shown efficacy in chemical castration by selectively targeting the reproductive system in rat models, their effects on other tissues cannot be overlooked. Following administration of Ag nanoparticles, they induce inflammation and oxidative damage at the site of injection. Furthermore, they may enter blood circulation and distribute to different body organs and trigger organ-specific pathophysiological effects<sup>35</sup>. However, Qin et al.<sup>36</sup> investigated the toxicological effects of silver nanoparticles in 100 rats following 28 days of oral administration at doses of 0.5 and 1 mg/kg body weight<sup>36</sup>. They found no significant toxic effects up to 1 mg/kg body weight, with respect to the body weight, organ weight, food intake, and histopathological examination. When rats were exposed to silver nanoparticles (AgNPs) and silver nitrate (AgNO<sub>3</sub>), the silver tended to accumulate in the same organs. The liver and kidneys were most affected, followed by the testes and spleen<sup>36</sup>. Carbon dots (CDs) can be easily eliminated from the body through urine. Because of their small size and neutral electrical charge, they can pass through the kidneys' filtering system without causing harm to organs like the spleen or liver. These unique properties make CDs promising tools for cancer treatment. They have been used successfully in medical imaging, delivering drugs and genes to cells, and using light to treat cancer cells (photothermal and photodynamic therapy)<sup>37</sup>. However, it is essential to balance these risks with the therapeutic benefits. In the context of chemical castration, the doses of Ag-CDs used are significantly lower than those that have been shown to cause toxicity in other studies. Moreover, our study utilized a short-term administration protocol, which is less likely to induce the chronic effects seen in other models. Nevertheless, we emphasize the importance of further research to establish the long-term safety profile of Ag-CDs, particularly focusing on their potential to induce systemic toxicity and their pharmacokinetic behavior.

## Conclusion

The present study demonstrated the role of Silver-Doped Carbon Dots in the rat model of chemical castration. Overall, AgCDs triggered a reduction in sperm concentration and histopathological parameters, oxidative damage, reduced fertility, and apoptosis, as indicated by changes in *P53*, *Bax*, *Bcl-2*, *caspase-3*, *AKT*, and *PI3K* expression levels. Further research is needed to determine the efficacy of AgCDs in chemical castration across other species.

## Methods

### Carbon dots production

Ag-doped CDs were synthesized through a hydrothermal procedure. Initially, 100 mL of an aqueous solution of citric acid monohydrate (0.8 g), urea (0.1 g), and AgNO<sub>3</sub> (0.1 g) was poured into a Teflon-lined stainless-steel autoclave and heated at 200 °C for four h. After cooling, the obtained solution was filtered with Whatman No. 1 filter paper and centrifuged at 14,000 rpm for 20 min, followed by dialysis utilizing a dialysis bag (MWCO: 1500 Da) for 48 h. Eventually, the purified solution was freeze-dried for storage and subsequent testing, with freezing temperatures maintained at −40 °C, pump pressure at 100 m Torr, and shelf temperature at −60 °C<sup>38</sup>.

### Animals and groups

30 male and 50 female Wistar albino rats weighing 250–300 g and approximate age of 12–14 weeks were utilized in this study. All animals were obtained from the animal resource department of Urmia University of Medical Sciences, Urmia, Iran. A controlled environment was provided with a temperature range of 20 ± 2 °C, a humidity of 50 ± 10%, and a day-night cycle of 12 h, each with suitable ventilation. All rats had free access to tap water and standard pellet. The Animal Ethics Committee of Urmia University approved the experiments and their guidelines were followed. All methods were performed in accordance with the relevant guidelines and regulations. Additionally, the current study adhered to the ARRIVE guidelines (Animals in Research: Reporting In Vivo Experiments). All rats ( $n=80$ ) were randomly divided into six equal groups, which had five males and ten females each, except the surgical group, which had only five males, as follows:

1. Control group: In this experimental group, rat testicles remained intact without any manipulation ( $n=15$ ).
2. Sham group: In this group, normal saline was injected into rat testicles ( $n=15$ ).
3. 1.25 AgCDs group: Silver carbon dots with a dosage of 1.25 µg/kg were injected into the caudal part of the testis toward the tail of the epididymis ( $n=15$ ).
4. 50 AgCDs group: Silver carbon dots with a dosage of 50 µg/kg were injected into the testis ( $n=15$ ).
5. 200 AgCDs group: Silver carbon dots with a dosage of 200 µg/kg were injected into the testis ( $n=15$ ).
6. Surgical group: 5 male rats were included in this group, which were surgically castrated only to measure the testosterone levels of the testes ( $n=5$ ).

No complications or death were observed during experiments. Eventually, on day 30, the animals were sacrificed using an overdose injection of thiopental sodium (250 mg/kg, IP)<sup>39</sup>. Sperm samples were taken from the tail of epididymis and blood samples were taken and centrifuged at 4 °C for 10 min at 2000 g. Subsequently, the serum was separated and kept at −80 °C until further analysis. Moreover, the left testicle in each group was separated and sorted at −80 °C for oxidative damage evaluation and the right testicle was maintained at 10% formalin buffer solution for histological assessments.

### Testosterone analyses

An enzyme-linked immunosorbent assay kit (Monobind Inc., Lake Forest, USA) was utilized to assess testosterone concentration according to the manufacturer's instructions. Control and serum samples (10 µL) were dispensed into the respective wells. Then, 100 µL testosterone-HRP conjugate was applied to each well, and a substrate blank was dispensed into well A1. The wells were covered with aluminum foil and incubated at room temperature for 1 h. Thereafter, the cover was removed, and the contents aspirated. Then, the wells were washed



three times with diluted HRP wash buffer, 300  $\mu\text{L}$  per well per wash, with a soaking time of about five seconds between each wash cycle. The remaining fluid was removed by tapping the strips on a paper towel. Subsequently, TMB (tetramethylbenzidine) substrate solution (100  $\mu\text{L}$ ) was added to all wells and the wells were incubated in a dark place for 15 min at room temperature. Stop solution (100  $\mu\text{L}$ ) was then applied to all wells in the same order and at the same rate as the substrate. Eventually, the absorbance was read at 450 nm within 20 min after adding the stop solution<sup>2</sup>.

## Sperm parameters assessment

### *Sperm motility*

The CASA system (Test sperm 3.2, Videotest, St. Petersburg, Russia) with a rat sperm setup was used to assess sperm concentration and kinetic parameters. Seven  $\mu\text{L}$  of sperm were placed in a chamber of slide-coverslip at a temperature of 37 °C. Then, a minimum of 500 cells were analyzed in the field at a 60-Hz frame rate. Typical cell sizes were 13 pixels, and sperms with a straightness of 50% and an average path velocity (VAP) of 50.0  $\mu\text{m}/\text{sec}$  were considered. Furthermore, the VAP cut-off and straight-line velocity cutoff were analyzed. For mean linearity below 38%, the curvilinear velocity was higher than 180  $\mu\text{m}/\text{sec}$ . The amplitude of lateral head displacement was set to exceed 9.5  $\mu\text{m}$  (Table 6). Sperm motility was assessed using a fraction of sperm suspension, approximately 10  $\mu\text{L}$ , placed on a microscopic slide. A dark or phase-contrast field microscope (Olympus, BX41, Tokyo, Japan) was used to observe a minimum of 500 spermatozoa across five microscopic fields<sup>40</sup>.

### *Sperm count*

Distilled water was used to dilute the sperms at a ratio of 1:5. Afterwards, a Neubauer hemocytometer (Brand™, Germany) was used to count spermatozoa. Epididymal tissue pieces were gathered and weighed cautiously utilizing a digital laboratory precision balance (Sartorius™, Japan) with a capacity of 0.0001 g. Eventually, the average number of epididymal sperm was reported as 10<sup>6</sup>/mL.

### *Sperm viability and morphology*

The eosin-nigrosin staining method was applied to assess sperm viability and morphology according to the World Health Organization protocol<sup>41</sup>. Eosin and nigrosin dyes (Merck, Darmstadt, Germany) were dissolved in distilled water. A light microscope (Model CHT, Olympus Optics Co. Ltd.) at a magnification of 400x was used to examine the mixture of one volume of sperm with two volumes of 1% eosin. Sperm viability was evaluated based on their coloring; viable sperms appeared red due to eosin staining, while non-viable sperms remained colorless. Similarly, eosin-nigrosin staining was used to determine the proportion of abnormal sperm. Sperm with discolored head, neck, or tail segments were considered non-viable. The abnormal sperm group had cytoplasmic remnants. Two hundred sperm from each sample were examined with 400 $\times$  magnification, and the results were recorded as a percentage<sup>40</sup>.

### *Sperm DNA damage*

The native, denatured, and double-stranded DNA in sperm chromatin was observed using Acridine orange (AO) staining. The denatured DNA demonstrated the highest fluorescent activity. Concentrated smears were soaked

Parameter	Setting
Frame rate	60-Hz
Number of frames	30
Duration of capture	1 s
Stage temperature rate	37 °C
Minimum cell size	4 pixels
Cell size	13 pixels
Minimum contrast	30
Cell intensity	75 pixels
Chamber type	Slide-Coverslip (22 $\times$ 22 mm)
Volume per slide	7 $\mu\text{L}$
Chamber depth	$\approx$ 20 $\mu\text{m}$
Minimum number of field analysis	500 cells
Image type	Phased contrast
Average path velocity (VAP)	50.0 $\mu\text{m}/\text{s}$
Straightness	50%
VAP cutoff	10.0 $\mu\text{m}/\text{s}$
Straight line velocity cutoff	0.0 $\mu\text{m}/\text{s}$
Curvilinear velocity	> 180 $\mu\text{m}/\text{s}$
Amplitude of lateral head	> 9.5 $\mu\text{m}$
Mean linearity	< 38%

**Table 6.** Parameter settings for the computer-assisted semen analysis.

in acetic acid (1:3) and Carnoy's fixative for 2 h and air dried for 5 min. The mixture was added to a stock solution of 1000 mL purified water and 1 mg AO and then stored in a dark room at 4 °C for 5 min. The spermatozoa were observed under a fluorescence microscope (Model GS7, Nikon Co., Tokyo, Japan) at a magnification of 400× after staining. Damaged or irregular spermatozoa were stained in red or yellow color<sup>40</sup>.

#### *Sperm plasma membrane functionality (PMF)*

The hypo-osmotic swelling test (HOST) is recognized as the PMF test. 10 µL of sperm sample was blended with 100 µL of a hypo-osmotic solution, including sodium citrate (0.735 g/L) and fructose (1.351 g/L). Subsequently, the mixture was incubated at 37 °C for 1 h. A phase contrast microscope (Olympus, BX41, Tokyo, Japan) at a magnification of 400× was employed to analyze the PMF. Coiled or swollen tails were the significant characteristics of an effective PMF<sup>40</sup>.

#### *Fertility indices assessment*

In all experimental groups except surgical group, five male and 10 female rats were included. Fertility indices including female mating index (%), male mating index (%), pregnancy index (%), and male fertility index (%) were measured.

#### *Evaluation of oxidative stress*

20–30 mg of testicular tissue was homogenized in 1000 µL of lysis buffer, then centrifuged at 9000 rpm for 15 min. Subsequently, the supernatant was used for biochemical analyses to evaluate enzymatic antioxidant activity. Navand Salamat commercial kits were used for all parameters in the present study (Navand Salamat Company, Urmia, Iran). Malondialdehyde (MDA) concentration was assessed using a commercial MDA assay kit. A spectrophotometer (Thermo Fisher Scientific; Waltham, MA) was used to assess the absorbance of samples using a 523 nm wavelength. The results were shown as nmol/g protein. A total antioxidant capacity (TAC) assay kit was employed to measure the levels of TAC in the testis. TAC results were shown as mmol/g protein. A glutathione peroxidase (GPx) kit, was used to measure the levels of GPx in the samples, and the final concentration of GPx was reported as U/mg protein. Levels of superoxide dismutase (SOD) in the testicular samples were evaluated using a SOD commercial kit. Moreover, the SOD activity was demonstrated according to the decrease in color development at 405 nm and it was reported as nmol/mg protein. A dichotomous protocol was applied to measure catalase (CAT) activity using a commercially available CAT kit. CAT activity was measured with an absorbance rate of 550 nm following a 10-min incubation at room temperature. The results were shown as U/mg protein. Levels of nitric oxide (NO) was measured using the NO commercial kit and the absorbance of samples were read at 570 nm. The final concentration of NO was reported as nmol/mg protein.

#### *Macroscopic and histopathological evaluation*

In all experimental groups, testis weight (g) and epididymis weight (g) were measured using a digital scale. Moreover, the percentage of Testis/body weight (%) was calculated.

The right testes of rats, kept in a 10% buffer formalin solution, were dehydrated using ethanol and then put in paraffin. Thin layers were cut using a rotary microtome with a seven µm width and stained using hematoxylin and eosin (H&E) stain. Thereafter, the stained slides were observed using a light microscope (Olympus Model BH-2, Tokyo, Japan). Two hundred randomly chosen round or approximately round cross-sections of seminiferous tubules were used to calculate seminiferous tubule diameter (STsD). A light microscopic ocular micrometer (Model CHT, Olympus Optical Co. Ltd., Tokyo, Japan) was used to measure the two vertical diameters of each cross-section. Their average values were then calculated. Additionally, the Sertoli Cell Index (SCI), the Reproductive Index (RI), and the Meiotic Index (MI) were measured using 60 seminiferous tubules randomly chosen per group. The SCI is the ratio of Sertoli cells, which have distinct nuclei and nucleolus, to the number of germ cells in seminiferous tubules. The RI measures the number of tubules with germ cells reaching at least middle or higher spermatogonial levels. The MI, the ratio of round spermatids to pachytene primary spermatocytes, indicates the number of cells lost during cell division. A calibrated ocular micrometer was used to measure the Leydig Cell Nuclear Diameter (LCND) according to the method described by Elias and Hyde<sup>42</sup>. The Tubular Differentiation Index (TDI) is defined as the number of seminiferous tubules with a minimum of three fully developed germ cells, and the Spermatogenic Index (SPI) is defined as the number of seminiferous tubules with sperm cells, were both determined by examining two hundred transverse sections of the seminiferous tubules from each animal (100 per testis).

The mean testicular biopsy score was evaluated to measure the spermatogenesis stage using the Johnsen scoring system, which grades 1 to 10<sup>43</sup>. Two hundred seminiferous tubules were assessed with a light microscope (CHT model, Olympus Optical Co. Ltd., Tokyo, Japan) (Table 7). The Cosentino's scoring system measured testicular damage<sup>44</sup>. This scoring system has four grades related to the tests. Grade 1 is regarded as the standard presentation of testis. Grade 2 represents nearly packed seminiferous tubules with less ordered, non-cohesive germ cells. Grade 3 indicates unkempt and shed germ cells with pyknotic and shrunk nuclei and indistinct borders of the seminiferous tubule. Grade 4 indicates seminiferous tubules are fully packed with germ cell coagulative necrosis.

#### **Quantitative reverse transcription polymerase chain reaction (qRT-PCR) assessment**

SinaSyber Blue HF-qPCR Mix (CinnaGen, Tehran, Iran) was utilized on a StepOne Real-Time PCR System (Applied Biosystems, USA) using a 25 µL reaction system and qRT-PCR technique. Moreover, the cDNA samples were used to measure the relative expression of the *Bax*, *P53*, *Caspase-3*, *AKT*, *PI3K*, and *Bcl-2* genes compared to the reference gene (*18SrRNA*). The qRT-PCR thermal cycle settings were adjusted as follows: A defatting cycle at 95 °C for 10 min, 45 three-step cycles each with 10 sec defatting at 95 °C, 30 sec compounding at 60 °C and

Johnsen score	Description of histological criteria
10	Full spermatogenesis
9	Slightly impaired spermatogenesis, many late spermatids, disorganized epithelium
8	Less than five spermatozoa per tubule, few late spermatids
7	No spermatozoa, no late spermatids, many early spermatids
6	No spermatozoa, no late spermatids, few early spermatids
5	No spermatozoa or spermatids, many spermatocytes
4	No spermatozoa or spermatids, few spermatocytes
3	Spermatogonia only
2	No germinal cells, Sertoli cells only
1	No seminiferous epithelium

**Table 7.** Johnsen scoring system used for testicular damage evaluation.

Gene name	Primer	Band size	References
<i>Bcl-2</i>	Forward: 5- CTCGTCGCTACCGTCGTCACT TCG-3	242 bp	46
	Reverse: 5- CAGATGCCGGTTCAGGTACTCAGTC-3		
<i>Bax</i>	Forward: 5- ACC AGC TCTGAACAGATC ATG-3	424 bp	46
	Forward: 5- TGG TCT TGGATCCAGACAAG-3		
<i>P53</i>	Forward: 5- CATCATCAGCTGGAAGACTC-3	378 bp	47
	Reverse: 5- TCAGCTCTCGGAACATCTC-3		
<i>Caspase-3</i>	Forward: 5- TGTCATCTCGCTCTGGTACG-3	279 bp	48
	Reverse: 5- AAATGACCCCTTCATCACCA-3		
<i>AKT</i>	Forward: 5- CACCTTTATCATCCGCTGCCT-3	140 bp	49
	Reverse: 5- TCGTCTCTTCTCCTGCCTCTT-3		
<i>PI3K</i>	Forward: 5- GGAGAACCTATTGCGAGGGAAG-3	171 bp	49
	Reverse: 5- AGGGAGCTGTAGAGTTGTAGG-3		
<i>18SrRNA</i>	Forward: 5- GCAATTATCCCATGAACG – 3 Reverse: 5- GGCCTCACTAAACCATCCAA- 3	123 bp	50

**Table 8.** Nucleotide sequences and product size of primers used in reverse transcription-polymerase chain reaction.

the stretching step at 72 °C for 30 sec. Calculating relative expression was done using gene expression in the samples by the following formula: Relative expression =  $2^{-(\Delta\Delta ct)}$ , where  $\Delta\Delta ct$  is derived by subtracting  $ct$  of the reference gene from  $ct$  of the tested gene and the  $\Delta ct$  values of  $ct$  are internal control samples. A logarithm of 10 of these numbers was employed to generate the normal distribution of the relative expression values and then evaluated<sup>45</sup>. Primers used in reverse transcription-polymerase chain reaction are provided in Table 8.

### Statistical analysis

The data was analyzed using SPSS software (version 26 for Windows, developed by SPSS Inc. in Chicago, IL, USA). To assess the distribution of the groups, a one-sample Kolmogorov-Smirnov test was performed. When the data followed a normal distribution, they were presented as the mean  $\pm$  standard error of the mean (SEM). For non-normally distributed data they were represented as the median and interquartile ranges. A one-way ANOVA was conducted for normally distributed data, followed by a Tukey post hoc test for further analysis. In cases where the data did not conform to normal distribution, a non-parametric Kruskal-Wallis test was employed to compare the groups. The threshold for statistical significance was set at  $p < 0.05$ .

### Data availability

The data that support the findings of this study are available from the corresponding author upon reasonable request.

Received: 26 June 2024; Accepted: 3 October 2024

Published online: 15 October 2024

### References

1. Abu-Ahmed, H. M. Chemical sterilization of dogs using single bilateral intra-testicular injection of calcium chloride or clove oil. *BMC Vet. Res.* **16**, 1–10 (2015).
2. Maadi, M. A. et al. Chemical castration using an intratesticular injection of mannitol: a preliminary study in a rat model. *Turk. J. Vet. Anim. Sci.* **45**, 519–530 (2021).

3. Ibrahim, A., Ali, M. M., Abou-Khalil, N. S. & Ali, M. F. Evaluation of chemical castration with calcium chloride versus surgical castration in donkeys: testosterone as an endpoint marker. *BMC Vet. Res.* **12**, 1–9 (2016).
4. Coetzee, J. F., Nutsch, A. L., Barbur, L. A. & Bradburn, R. M. A survey of castration methods and associated livestock management practices performed by bovine veterinarians in the United States. *BMC Vet. Res.* **6**, 1–19 (2010).
5. Khatri Shweta, P., Suthar, B., Desai, R., Nakashi, H. & Sindhi, P. Ultrasonographic alterations in testes of rat following chemical sterilization with bilateral intra testicular injection of calcium chloride. (2022).
6. Spruijt, A. et al. The function of the pituitary-testicular axis in dogs prior to and following surgical or chemical castration with the GnRH-agonist deslorelin. *Reprod. Domest. Anim.* **58**, 97–108 (2023).
7. Abou-Khalil, N. S., Ali, M. F., Ali, M. M. & Ibrahim, A. Surgical castration versus chemical castration in donkeys: response of stress, lipid profile and redox potential biomarkers. *BMC Vet. Res.* **16**, 1–10 (2020).
8. Hami, M., Veshkini, A., Jahandideh, A., Rafiee, S. M. & Mortazavi, P. Evaluation of Testosterone, Blood antioxidants, and histopathological changes following Chemical Castration with Calcium Chloride in rats. *Crescent J. Med. Biol. Sci.* **9** (2022).
9. Zedan, I. A. & Al-Badrany, M. S. T. Control of stray dog population by single intratesticular injection of tannic acid. *Iraqi J. Vet. Sci.* **35**, 33–36 (2021).
10. Dayanti, M. D., Berata, I. K. & Puja, I. K. Sperm quality and histology of the testis and epididymis in chemical castrated male cats with intra-testicular injection of sodium chloride solution. *World's Vet. J.* **11**, 634–641 (2021).
11. Abshenas, J., Molaie, M. M., Derakhshfar, A. & Ghalekhani, N. Chemical sterilization by intratesticular injection of eugenia caryophyllata essential oil in dog: a histopathological study. *Iran. J. Vet. Surg.* **8**, 9–16 (2013).
12. Moustafa, S., Hassanein, K., Abdou, M., Fadl, L. R. & Sabra, M. S. Chemical castration with formalin versus surgical castration in dogs: hormonal, seminal fluid, cellular stress response, and testicular tissue alterations. *Assiut Vet. Med. J.* **69**, 69–87 (2023).
13. Tejwan, N. et al. Metal-doped and hybrid carbon dots: a comprehensive review on their synthesis and biomedical applications. *J. Control. Release.* **330**, 132–150 (2021).
14. Azam, N., Ali, N., Javaid Khan, T. & M. & Carbon quantum dots for biomedical applications: review and analysis. *Front. Mater.* **8**, 700403 (2021).
15. Gao, W. et al. Carbon dots with red emission for sensing of Pt<sup>2+</sup>, Au<sup>3+</sup>, and Pd<sup>2+</sup> and their bioapplications in vitro and in vivo. *ACS Appl. Mater. Interfaces.* **10**, 1147–1154 (2018).
16. Truskewycz, A. et al. Carbon dot therapeutic platforms: administration, distribution, metabolism, excretion, toxicity, and therapeutic potential. *Small.* **18**, 2106342 (2022).
17. Chan, M. H. et al. Natural carbon nanodots: toxicity assessment and theranostic biological application. *Pharmaceutics.* **13**, 1874 (2021).
18. Long, C. et al. Applications of carbon dots in environmental pollution control: a review. *Chem. Eng. J.* **406**, 126848 (2021).
19. Ezati, P., Rhim, J. W., Molaie, R., Priyadarshi, R. & Han, S. Cellulose nanofiber-based coating film integrated with nitrogen-functionalized carbon dots for active packaging applications of fresh fruit. *Postharvest. Biol. Technol.* **186**, 111845 (2022).
20. Rosenkrans, Z. T. et al. Selenium-doped carbon quantum dots act as broad-spectrum antioxidants for acute kidney injury management. *Adv. Sci.* **7**, 2000420 (2020).
21. Da Cunha, I., de Ascencao Rocha, A., Quirino, C. & Gimenes, A. The efficacy of in vitro sperm tests in predicting pregnancy success after artificial insemination in the bitch. *Androl. (Los Angel)*. **6**, 2167–20250 (2017).
22. Jung, H. & Yoon, M. Effects of intratesticular injection of 70% glycerin on stallions. *J. Equine Vet. Sci.* **49**, 1–10 (2017).
23. Pereira, R., Sá, R., Barros, A. & Sousa, M. Major regulatory mechanisms involved in sperm motility. *Asian J. Androl.* **19**, 5–14 (2017).
24. Mohammed, A. & James, F. Chemical castration by a single bilateral intra-testicular injection of chlorhexidine gluconate and cetrимide in bucks. *Sokoto J. Vet. Sci.* **11**, 62–65 (2013).
25. Oliveira, E. C. et al. Permanent contraception of dogs induced with intratesticular injection of a zinc gluconate-based solution. *Theriogenology.* **77**, 1056–1063 (2012).
26. Ahavan, O. et al. Influence of heavy nanocrystals on spermatozoa and fertility of mammals. *Mater. Sci. Eng. C.* **69**, 52–59 (2016).
27. Havrdova, M. et al. Toxicity of carbon dots—effect of surface functionalization on the cell viability, reactive oxygen species generation and cell cycle. *Carbon.* **99**, 238–248 (2016).
28. Habiba, K. et al. Synergistic antibacterial activity of PEGylated silver–graphene quantum dots nanocomposites. *Appl. Mater. Today.* **1**, 80–87 (2015).
29. Asharani, P., Wu, Y. L., Gong, Z. & Valiyaveetil, S. Toxicity of silver nanoparticles in zebrafish models. *Nanotechnology.* **19**, 255102 (2008).
30. Borovaya, M. et al. Synthesis, properties and bioimaging applications of silver-based quantum dots. *Int. J. Mol. Sci.* **22**, 12202 (2021).
31. Emir, L. et al. *Urologic Oncology: Seminars Original Investigations* 392–396 (Elsevier).
32. Karami, N., Veshkini, A., Asghari, A., Rafiee, S. M. & Mortazavi, P. The pathological and ultrasonographic evaluation of the chemical castration in dogs using calcium chloride injection. *Arch. Razi Inst.* **78**, 1579 (2023).
33. Kwak, B. K. & Lee, S. H. Intratesticular injection of hypertonic saline: non-invasive alternative method for animal castration model. *Dev. Reprod.* **17**, 435 (2013).
34. De Macedo, S. R. B. et al. Effects of intratesticular injection of zinc-based solution in rats in combination with anti-inflammatory and analgesic drugs during chemical sterilization. *Vet. World.* **11**, 649 (2018).
35. Ferdous, Z. & Nemmar, A. Health impact of silver nanoparticles: a review of the biodistribution and toxicity following various routes of exposure. *Int. J. Mol. Sci.* **21**, 2375 (2020).
36. Qin, G. et al. Toxicological evaluation of silver nanoparticles and silver nitrate in rats following 28 days of repeated oral exposure. *Environ. Toxicol.* **32**, 609–618 (2017).
37. Ullah, I. et al. An insight into recent developments of copper, silver and gold carbon dots: cancer diagnostics and treatment. *Front. Bioeng. Biotechnol.* **11**, 1292641 (2023).
38. Zhuo, S. J., Fang, J., Wang, J. & Zhu, C. Q. One-step hydrothermal synthesis of silver-doped carbon quantum dots for highly selective detection of uric acid. *Methods Appl. Fluoresc.* **8**, 015005 (2019).
39. Davoodi, F. et al. Investigating the sperm parameters, oxidative stress and histopathological effects of salvia miltiorrhiza hydroalcoholic extract in the prevention of testicular ischemia reperfusion damage in rats. *Theriogenology.* **144**, 98–106 (2020).
40. Ramazani, N. et al. The influence of L-proline and folic acid on oxidative stress and semen quality of buffalo bull semen following cryopreservation. *Vet. Med. Sci.* **9**, 1791–1802 (2023).
41. Organization, W. H. Department of reproductive health and research. *WHO Lab. Man. Exam. Process. Hum. Semen.* **5**, 21–22 (2010).
42. Elias, H. & Hyde, D. M. An elementary introduction to stereology (quantitative microscopy). *Am. J. Anat.* **159**, 411–446 (1980).
43. Johnsen, S. G. Testicular biopsy score count—a method for registration of spermatogenesis in human testes: normal values and results in 335 hypogonadal males. *Hormone Res. Paediatr.* **1**, 2–25 (1970).
44. Cosentino, M. J., Nishida, M., Rabinowitz, R. & Cockett, A. T. Histopathology of prepubertal rat testes subjected to various durations of spermatic cord torsion. *J. Androl.* **7**, 23–31 (1986).
45. Soleimanzadeh, A., Pourebrahim, M., Delirez, N. & Kian, M. Ginger ameliorates reproductive toxicity of formaldehyde in male mice: evidences for Bcl-2 and Bax. *J. Hermed. Pharmacol.* **7**, 259–266 (2018).



46. Taghavi, S. A., Valojerdi, M. R., Moghadam, M. F., & Ebrahimi, B. Vitriification of mouse preantral follicles versus slow freezing: Morphological and apoptosis evaluation. *Anim. Sci. J.* **86**(1), 37–44. <https://doi.org/10.1111/asj.12244> (2015).
47. Sheikhbahaei, F., Khazaei, M., Rabzia, A., Mansouri, K., & Ghanbari, A. Protective effects of thymoquinone against methotrexate-induced germ cell apoptosis in male mice. *Int. J. Fertil. Steril.*, **9**(4), 541 (2016).
48. Han, X., Ge, R., Xie, G., Li, P., Zhao, X., Gao, L., Zhang, H., Wang, O., Huang, F., & Han, F. Caspase-mediated apoptosis in the cochleae contributes to the early onset of hearing loss in A/J mice. *ASN Neuro.* **7**(1), 1,759,091,415,573,985 (2015).
49. Dhulqarnain, A. O., Takzaree, N., Hassanzadeh, G., Tooli, H., Malekzadeh, M., Khanmohammadi, N., Yaghobinejad, M., Solhjoo, S., & Rastegar, T. Pentoxifylline improves the survival of spermatogenic cells via oxidative stress suppression and upregulation of PI3K/AKT pathway in mouse model of testicular torsion-detorsion. *Heliyon.* **7**(4) (2021).
50. Soleimanzadeh, A., Kian, M., Moradi, S., & Mahmoudi, S. Carob (*Ceratonia siliqua* L.) fruit hydro-alcoholic extract alleviates reproductive toxicity of lead in male mice: Evidence on sperm parameters, sex hormones, oxidative stress biomarkers and expression of Nrf2 and iNOS. *Avicenna J. Phytomed.* **10**(1), 35 (2020).

## Acknowledgements

The authors want to appreciate the members of the Faculty of Veterinary Medicine and Urmia University Research Council and Dr. Ali Shalazar-Jalali (Associate Professor of Comparative Histology, Faculty of Veterinary Medicine, Urmia University) for his valuable advice on histological assessments.

## Author contributions

AS: Investigation, project administration, methodology, conceptualization, formal analysis, writing—review and editing. NK: Methodology, conceptualization, writing—original draft. FD: Investigation, methodology, conceptualization, supervision, writing—original draft. RM: Conceptualization, data curation, writing—review and editing, validation. AR: Investigation, methodology, writing—review & editing, visualization.

## Funding

This work was supported by Vice chancellor of Research and Technology of Urmia University.

## Declarations

## Competing interests

The authors declare no competing interests.

## Ethics approval and consent to participate

The Animal Ethics Committee of Urmia University approved the experiments and their guidelines were followed (IR-UU-AEC-3/20). Additionally, the current study adhered to the ARRIVE guidelines (Animals in Research: Reporting In Vivo Experiments).

## Additional information

**Correspondence** and requests for materials should be addressed to A.S. or F.D.

**Reprints and permissions information** is available at [www.nature.com/reprints](http://www.nature.com/reprints).

**Publisher's note** Springer Nature remains neutral with regard to jurisdictional claims in published maps and institutional affiliations.

**Open Access** This article is licensed under a Creative Commons Attribution-NonCommercial-NoDerivatives 4.0 International License, which permits any non-commercial use, sharing, distribution and reproduction in any medium or format, as long as you give appropriate credit to the original author(s) and the source, provide a link to the Creative Commons licence, and indicate if you modified the licensed material. You do not have permission under this licence to share adapted material derived from this article or parts of it. The images or other third party material in this article are included in the article's Creative Commons licence, unless indicated otherwise in a credit line to the material. If material is not included in the article's Creative Commons licence and your intended use is not permitted by statutory regulation or exceeds the permitted use, you will need to obtain permission directly from the copyright holder. To view a copy of this licence, visit <http://creativecommons.org/licenses/by-nc-nd/4.0/>.

© The Author(s) 2024